Sensors & Actuators: B. Chemical 299 (2019) 126972

Contents lists available at ScienceDirect

Sensors and Actuators B: Chemical

journal homepage: www.elsevier.com/locate/snb

Fuel cell type H_2S sensor utilizing Pt-Sn-C/Nafion sensing electrode

Xinyu Yang, Weijia Li, Yueying Zhang, Tong Liu, Xidong Hao, Ri Zhou, Xishuang Liang*, Fengmin Liu, Fangmeng Liu, Yuan Gao, Xu Yan, Geyu Lu*

State Key Laboratory on Integrated Optoelectronics, College of Electronic Science and Engineering, Jilin University, 2699 Qianjin Street, Changchun 130012, China

ARTICLE INFO

Keywords:
H_2S sensor
Nafion
Pt-Sn/C
Room-temperature
Fast response-recovery

ABSTRACT

A Nafion-based amperometric sensor utilizing Pt-Sn/C sensing electrode was developed to realize the effective detection of H_2S at room temperature. We compared the morphology and gas-sensing properties of two kinds of Pt/C materials prepared by the sodium borohydride reduction method and the ethylene glycol method and found that the latter was significantly better. Pt-Sn/C prepared by the latter method has a uniform morphology and high catalytic activity and achieves efficient detection of H_2S. The sensor could detect 0.2–100 ppm H_2S linearly with a sensitivity of 0.276 μA/ppm. More importantly, the response-recovery time to 50 ppm H_2S was 10 s and 8 s, which signified a very fast rate. Furthermore, the device also exhibited superior selectivity and long-term stability. Such a device has a good application prospect because of its many advantages.

1. Introduction

Hydrogen sulfide (H_2S), as one of the most common toxic gases, is mainly found in oil fields, sewage wells, volcanic gas, natural gas, and well water [1,2]. As a strong neurotoxic agent, H_2S is colorless, flammable, corrosive, and with the especial foul smell of rotten eggs [3]. When the human body inhales H_2S into the respiratory tract, the mucous membrane will be strongly stimulated, and even the central nervous system will be deprived of oxygen, causing serious consequences such as suffocation, which poses a great threat to human health [4]. According to the standards of OSHA, 10 ppm is the permissible exposure limit and 20 ppm is the acceptable ceiling concentration. Therefore, it is important to develop a portable and fast-responding H_2S sensor with high selectivity, stability, and sensitivity.

At present, most of the sensors for detecting H_2S use metal oxide semiconductors as sensing materials, such as ZnO [5,6], SnO_2 [7,8], CuO [9], MoO_3 [10], and Fe_2O_3 [11]. Such sensors are low in cost, small in size, and high in sensitivity, but they also have disadvantages such as poor selectivity and slow recovery. In order to improve selectivity, composite metal oxide semiconductors have gradually attracted the attention of researchers. By synthesizing $CuWO_4$ and NiO supported by SnO_2, Stanoiu et al. [12] and Kaur et al. [13] greatly improved the selectivity of the sensor while ensuring high sensitivity. The CuO-In_2O_3-based sensor reported by Lee et al. [14] responded to 5 ppm H_2S by as much as 1.16×10^5 at 150 °C, while the responses to other interfering gases were negligible. Yeh et al. [15] used CuO nanoparticles modified V_2O_5 nanowires to greatly reduce the response to interfering gases CO and NO_2. However, the response and recovery time of such sensors is still relatively long, making it difficult to achieve real-time detection of H_2S. There is also a class of H_2S sensors that use optical or photoacoustic principles. They have high detection accuracy, but the structure is complex and bulky and thence it is also difficult to realize portable and real-time detection of H_2S [16–18]. Therefore, it is necessary and urgent to develop an intrinsically safe, fast response-recovery H_2S sensor with high selectivity, sensitivity, and stability.

Nafion is a proton exchange membrane invented by DuPont Co. in the late 1960s. The proton conducting channels are formed inside the Nafion membrane when it is sufficiently hydrated so that the Nafion exhibits high proton conductivity [19]. Due to the chemical and mechanical stability, Nafion is widely used as the electrolyte in PEMFC. In recent years, amperometric gas sensors based on Nafion have been widely reported. The detection principle of this type of sensor is shown in Fig. 1. The gas to be tested reacts electrochemically at the anode side. The protons generated can transfer to the cathode side through the Nafion membrane, while, the electrons can only transfer through an external circuit. Afterward, protons and electrons react with oxygen to form water at the cathode side. Therefore, the concentration of the gas to be measured can be obtained by detecting the value of the short-circuit current. No bias voltage is applied to the whole process, and a current signal can be generated as long as the gas enters. Mochizuki et al. used this principle to prepare an amperometric CO sensor, which achieved linear detection in the range of 0–3000 ppm without applied voltage [20]. Rahman et al. used this structure to study the application of power-generating fuel cell electrode materials and monitoring

* Corresponding authors.
E-mail addresses: liangxs@jlu.edu.cn (X. Liang), lugy@jlu.edu.cn (G. Lu).

https://doi.org/10.1016/j.snb.2019.126972
Received 11 April 2019; Received in revised form 3 July 2019; Accepted 12 August 2019
Available online 14 August 2019
0925-4005/

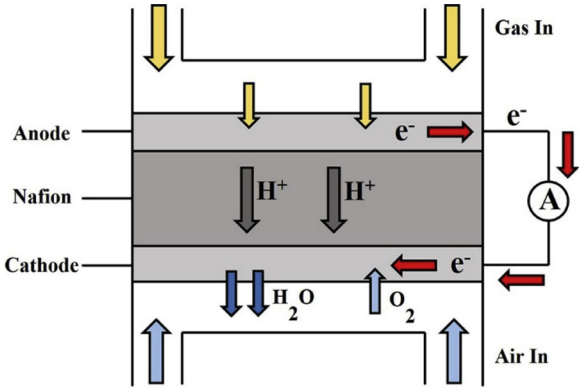

Fig. 1. Schematic diagram of a fuel cell type sensor.

methods to breath alcohol sensor [21]. Compared with the resistive sensor, this working mode without applied voltage avoids polarization, reduces power consumption, and has a simple structure and accurate output signal. Based on the above foundation, our research group reported an amperometric CO sensor and got good results [22,23]. This new type of amperometric gas sensor has the advantages of zero power consumption, environmental friendliness, and intrinsic safety, which has attracted increasing attention from researchers. Currently reported Nafion-based gas sensors are mainly used to detect alcohol [21,24], CO [20,25], SO_2 [26], NO [27,28], NO_2 [29], O_2 [30,31], and H_2 [32–34], but there are very few reports on H_2S. Therefore, Nafion-based high-performance H_2S sensors are well worth studying.

In our previous work, Pt-Rh/C was used as an electrode material to detect H_2S and achieved good performance [35]. The sensor had a sensitivity of 0.191 μA/ppm and had good selectivity. Carbon was used as a support in the electrode material, which is widely used in the preparation of PEMFC catalysts. On the one hand, the use of carbon can reduce the amount of precious metal used, and more importantly, the carrier affects the dispersion, stability, and utilization of the catalyst, which is an indispensable part. Carbon fiber (CF) used in this work is resistant to high temperature, corrosion, creep and excellent electrical conductivity. Therefore, we chose it as a carrier to prepare sensing electrode materials with a loose structure and high stability. Moreover, in the work of Guan et al. [23], CF has also proven to be the best support. However, there are also disadvantages that metal nanoparticles (NPs) are easy to aggregate and costly. In order to obtain a better morphology, increase the sensitivity of the sensor and reduce the manufacturing cost of the sensor, in this article, we improved the preparation method and replaced Rh with a relatively inexpensive and readily available Sn. The reason why Sn is chosen mainly is based on the following three aspects. First, Sn is a commonly used gas sensitive material. There have been many reports on the modification of Sn in materials to improve the gas sensing performance [36–38]. Second, it has been reported in the literature that Pt-Sn is applied to the catalytic oxidation of methanol [39,40], ethanol [41,42], and the dehydrogenation of propane [43,44]. We speculate that the application of this material to H_2S detection can also get better performance. Third, according to Gwebu et al. [45], the incorporation of Sn does not adversely affect Pt but rather increases the catalytic activity of the material.

In González-Quijano and López-Suárez's works [46,47], they reported the effects of specific experimental parameters on the catalytic oxidation of ethanol in the process of preparing Pt-Sn/C using the ethylene glycol process. While, in this work, we compared the materials prepared by the ethylene glycol method with the sodium borohydride reduction method and found that the former was significantly better. Next, we fabricated a Nafion-based fuel cell type H_2S sensor using Pt-Sn/C prepared by ethylene glycol method and studied the gas sensing characteristic in detail. Such bimetallic catalyst is capable of improving the poor selectivity of a single Pt catalyst. We characterized the prepared electrode material and analyzed the sensitive mechanism of the sensor, and discussed the sensing properties. It was found that it exhibited superior selectivity, high sensitivity, fast response-recovery rate, and good long-term stability.

2. Experimental

2.1. Electrode material synthesis

Pt-Sn NPs supported on CFs were synthesized following the ethylene glycol method [48,49]. Appropriate amounts of $PtCl_4$ (Aikeda Chemical Reagent Co., Ltd.) and $SnCl_2$ (Xiqiao Chemical Co., Ltd.) were weighed into a beaker, wherein the weight ratio of Pt and Sn was 1:1. Adding a certain amount of CFs (Kejing Carbon Fiber Co., Ltd.) made the weight ratio of CFs to metal 4:1. Then, ethylene glycol (Beijing Chemical Works) was poured into the beaker as a solvent and a reducing agent. The suspension was thoroughly stirred at room temperature and the pH was adjusted to 11. Next, raised the temperature to 160 °C under an N_2 atmosphere and then reacted for 3 h. After that, the mixture was filtered and dried at 80 °C and treated under N_2 flow for 1 h at 250 °C. The prepared catalyst was labeled as Pt-Sn/C (EM_c). Two kinds of 10% Pt/C prepared using sodium borohydride reduction method [35] and ethylene glycol method were used for comparison, labeled as EM_a and EM_b.

2.2. Sensor fabrication

Fig. 2(a) is the schematic diagram of the fabricated device. It comprises a gas diffusion cap, a membrane electrode assembly (MEA, including sensing electrode, Nafion membrane, and counter electrode), an isolation disc, and a water container. H_2S diffuses into the interior of the sensor from the pores of the cap and electrochemically reacts on the MEA. The water in the container is used to maintain the humidity required for the Nafion membrane to function properly. MEA, the core part of this sensor, its preparation process can be found in our previous work [35]. Fig. 2(b) is the actual image of the device. Sensors fabricated using EM_a, EM_b, and EM_c were labeled as S_a, S_b, and S_c, respectively.

The crystalline structure was analyzed using X-ray diffractometer

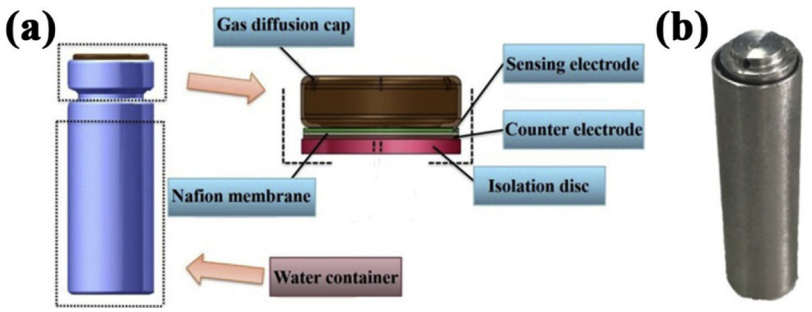

Fig. 2. (a) Schematic diagram of the fabricated sensing device; (b) The actual image of the device.

(Rigaku wide-angle X-ray diffractometer with CuKα radiation at 0.1541 nm, 0.2°/s). Field emission scanning electron microscope (JEOL JSM-2100 F) and high-resolution transmission electron microscope (JEOL JEM-2100 F) operated at 200 kV were used to observe the surface morphology. Energy dispersive spectrometer (EDS, TEDS-X0100TLE) was used to study element distribution and content of the catalyst powder.

Electrochemical workstation (CHI611C, Shanghai Instrument Corporation, China) was used to study the sensing performance. In order to get different concentrations of H_2S, we diluted a certain amount of 1% H_2S with air in a bottle. The short-circuit current of the sensor is I_a in air and I_b in H_2S. We define the difference between I_a and I_b as the response current (ΔI). ΔI-t curves of this H_2S sensor were measured without giving a potential between the anode and cathode. The response and recovery times are defined as the time required to reach 90% value of ΔI. The sensitivity is defined as the slope of the line fitted by ΔI and H_2S concentration. All results were obtained under laboratory condition.

3. Results and discussion

Fig. 3 shows the X-ray diffraction patterns of the prepared materials. For EM_a and EM_b, the diffraction peaks located at 2θ = 39.8°, 46.3°, 67.5°, 81.3°, and 85.7° correspond to the Pt cubic structure (JCPDS Card No. 4-802). It is worth noting that the characteristic peaks of EM_b are wider, indicating that the particle size of the metal NPs is smaller. For EM_c, it can be seen that the catalyst is a multiphase component, including Pt, Pt_3Sn and a small amount of SnO_x. These results are consistent with reports by Roca-Ayats and López-Suárez et al. [47,48]. According to Antolini et al. [50], the coexistence of different Pt-Sn phases may not weaken the performance of the catalyst, and conversely, even increase the activity.

The morphology of the above electrode materials is shown in Fig. 4. Fig. 4(a), (c) and (e) are the FESEM images of EM_a, EM_b and EM_c, and Fig. 4(b), (d) and (f) are the HRTEM images of EM_a, EM_b, and EM_c, respectively. From Fig. 4(a) and (b) we can see that the agglomeration of Pt NPs was very serious and most of the CFs surface was exposed, and few particles were carried on it. The average size of the Pt NPs was 5.3 nm. For EM_b, the agglomeration of Pt NPs was significantly improved, and Pt NPs were uniformly supported on the surface of CFs as shown in Fig. 4(d). The average size was 3.2 nm. For EM_c, as shown in Fig. 4(e) and (f), the surface of CFs was uniformly covered with Pt-Sn NPs, and the surface was rougher than EM_b, in which more active sites

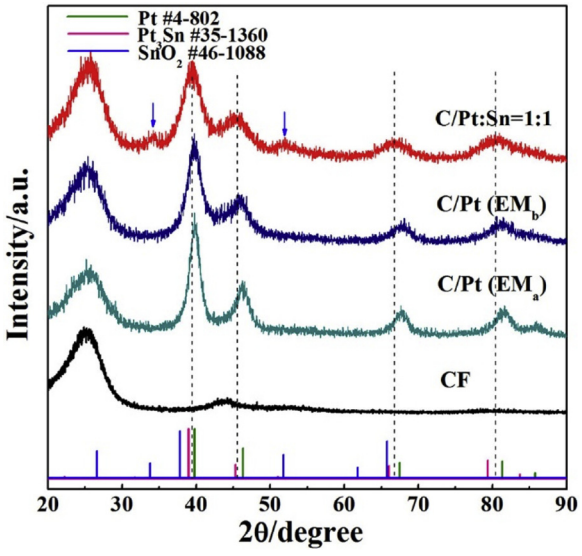

Fig. 3. XRD patterns of sensing materials synthesized.

were exposed. The average size of the Pt-Sn NPs was 3.2 nm, which was consistent with the results obtained in the XRD patterns. We also used EDS to study the element distribution of the electrode materials and the results are shown in Fig. 5. It can be seen from Fig. 5(a) to (c) that the aggregation of Pt NPs in EM_a is very serious, while, in EM_b, the distribution of particles had been greatly improved. Furthermore, the EDS measurement confirmed that the C, Pt and Sn elements were coexisting and uniformly dispersed in Fig. 5(g)–(j). According to Rodríguez's work [51], the polyol method would assure a stronger interaction between the support and the metallic precursor during the deposition-reduction in the liquid phase, leading to higher dispersions of the metallic phase. Therefore, we obtained NPs with smaller particle size and more uniform distribution by ethylene glycol method, which is obviously superior to sodium borohydride reduction method.

In order to clarify the effect of the added Sn on the microstructure and sensing performance of the electrode material, we performed BET tests on EM_b and EM_c. It can be seen from Table 1 that the BET surface area of EM_c is nearly 4 times larger than that of EM_b. In other words, the addition of Sn significantly increases the surface area of the material, which means that more active sites are exposed, and it will increase the sensitivity of the sensor.

To examine the sensitivities of S_a, S_b, and S_c, we measured the response currents of these sensors to 1–50 ppm H_2S and the results are shown in Fig. 6. The sensitivity of S_c is the highest, reaching 0.276 μA/ppm, followed by S_b, and finally S_a, only 0.168 μA/ppm. These results are in good agreement with our speculation.

Here, we analyze the sensing mechanism of the sensor. According to the report by Gaidi et al. [52], the possible oxidation reactions of H_2S on the sensing electrode side are as follows:

$$Pt\text{-}H_2S_{ads.} \rightarrow Pt\text{-}SH_{ads.} + H^+ + e^- \quad (1)$$

$$Pt\text{-}SH_{ads.} \rightarrow Pt\text{-}S_{ads.} + H^+ + e^- \quad (2)$$

Due to the presence of SnO_x, the following reactions are equally likely to occur [53]:

$$O_{2(g)} + 2e^- \rightarrow 2O^-_{(ads)} \quad (3)$$

$$H_2S_{(g)} + 3O^-_{(ads)} \rightarrow SO_{2(g)} + H_2O_{(g)} + 3e^- \quad (4)$$

The reaction on the counter electrode is as follows:

$$2H^+ + 1/2O_2 + 2e^- \rightarrow H_2O \quad (5)$$

Protons generated by the reaction on the sensing electrode side are transported to the counter electrode through the Nafion, and electrons can only be transported through the external circuit. Thus, the short circuit current of the sensor corresponds to the concentration of H_2S.

The highest sensitivity of Pt-Sn/C is mainly due to the following three reasons. First, a uniform morphology ensures good contact of the electrode material with the Nafion membrane, allowing protons and electrons produced by reactions (1)-(4) to pass smoothly. Second, the bimetallic electrode material has a higher catalytic activity than pure Pt. Rodríguez et al. [51] examined the electrochemical active surface (EAS) and H_2 chemisorption values of the above three materials (Pt/C ($NaBH_4$), Pt/C (EG), Pt-Sn/C (EG)) and found that the Pt-Sn/C prepared by the ethylene glycol method has the highest value. This may be due to a decrease in particle size and the presence of geometrical/electronic effects of the promoter on Pt site. At the meanwhile, this catalyst has a good CO tolerance and important stability determined by chronoamperometry measurements. Gwebu et al. [45] conducted a series of electrochemical tests and proved that the Pt-Sn/C electrocatalyst exhibited high current densities and lower poisoning rates compared to the Pt/C. On the other hand, the addition of Sn makes the reactions (3), (4) happen, and the resulting electrons also contribute to the increase in sensitivity. Third, the multiphase components including Pt, Pt_3Sn, and SnO_2 also contribute to the catalytic activity of the electrode material. Antolini et al. proposed a model validated by experimental data to

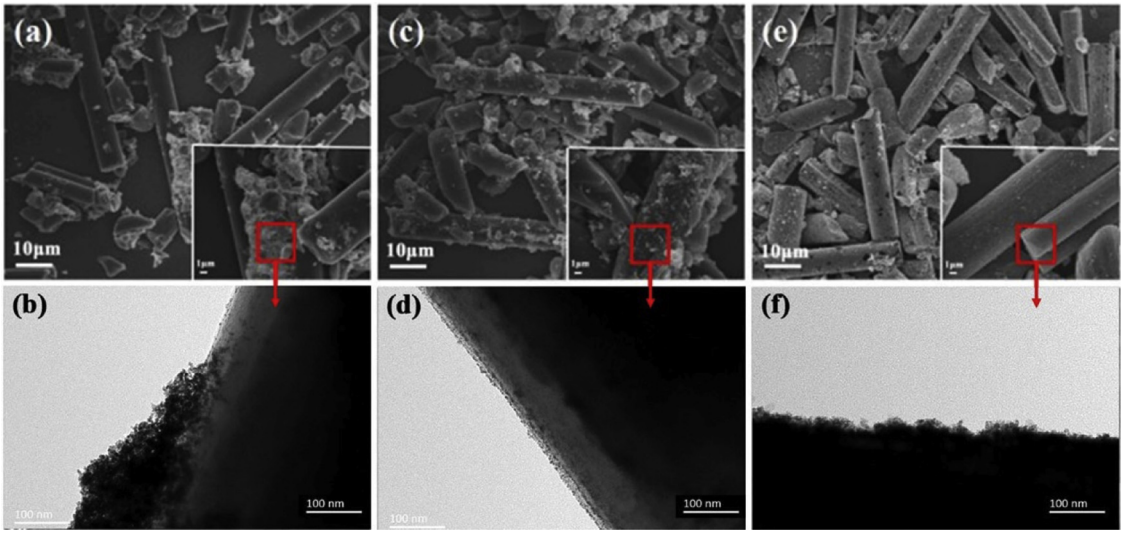

Fig. 4. FESEM and TEM images of EM_a ((a), (b)), EM_b ((c), (d)), and EM_c ((e), (f)).

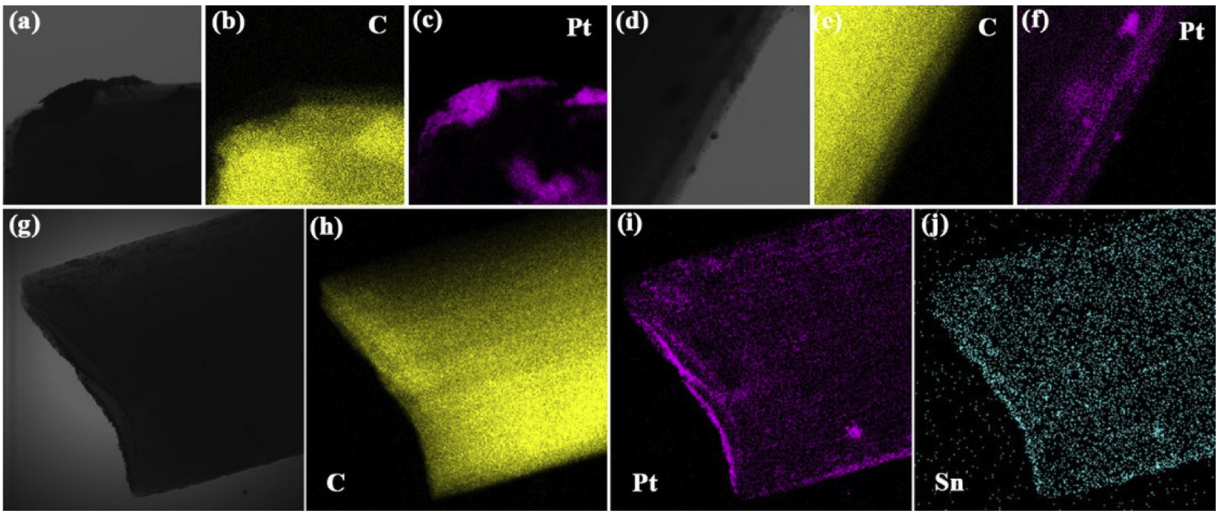

Fig. 5. EDS mapping images of EM_a ((a)–(c)), EM_b ((d)–(f)), and EM_c ((g)–(j)).

Table 1
The BET surface areas and average pore diameters of EM_b and EM_c.

Sample	BET Surface Area(m^2/g)	Average Pore Diameter(nm)
EM_b	2.99	23.78
EM_c	11.77	9.14

predict the performance of a single direct ethanol fuel cell by varying the degree of alloying of the Pt-Sn/C catalyst used as the anode material. For partially alloyed catalysts (Pt_zSn phase alloy and Pt-SnO_x), the model predicts a maximum MPD (maximum power density), which will be more beneficial to the gas catalytic reaction. Besides, Ghimbeu and Dong et al. reported SnO_2-based and Pt-SnO_2-based H_2S sensors and the sensors showed good performance, including high response and fast recovery time [54,55], which indicates that the presence of SnO_2 in our multi-system materials may contribute to the catalytic reaction of H_2S. Although multiphase mixed Pt-Sn/C catalysts (including Pt, Pt_3Sn, and SnO_2) are usually obtained using the polyol method [56–58], we have achieved high sensitivity detection of H_2S using the multiphase components of the catalyst, which is exactly what we want. In summary, we believe that prepared Pt-Sn/C is the best sensing electrode material. Next, the detailed gas-sensing properties of S_c were investigated.

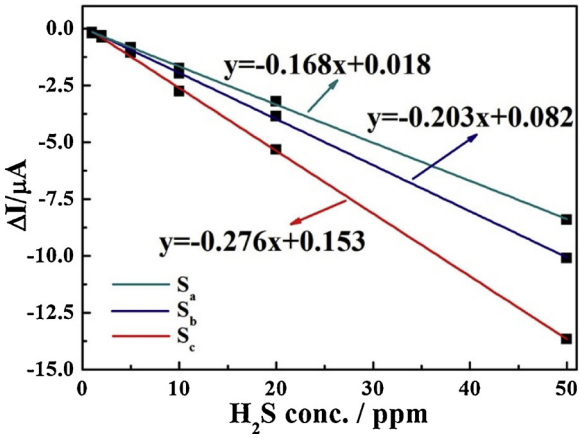

Fig. 6. Comparison of the sensitivity curves for S_a, S_b, S_c.

Fig. 7(a) shows the response-recovery curves to different H_2S concentrations. The sensor was placed in the air and H_2S for both 200 s. It is obvious that ΔI increases as the concentration of H_2S increases. When the concentration of H_2S is 50 ppm or less, ΔI can reach a stable value. When it reaches 100 ppm, ΔI continues to drop and cannot reach a

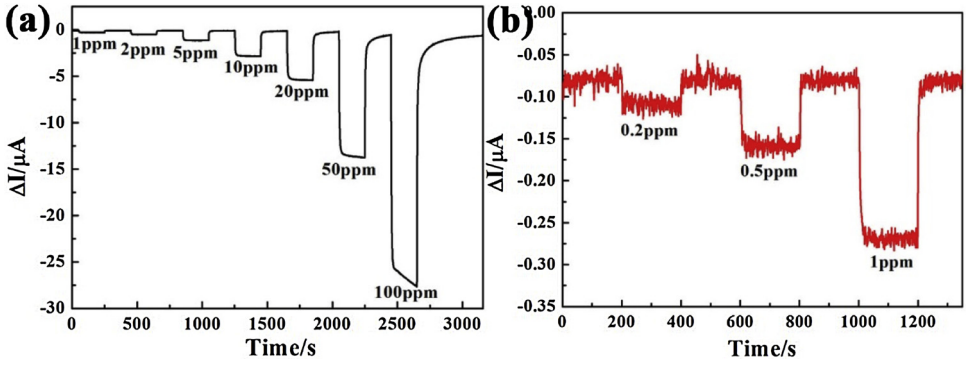

Fig. 7. The typical response transients to different concentrations of H_2S in the range of (a) 1–100 ppm and (b) 0.2–1 ppm.

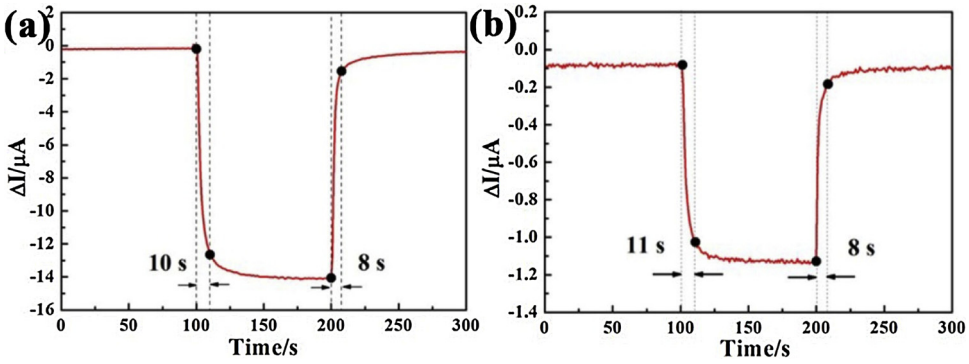

Fig. 8. The typical response transient of S_c to (a) 50 ppm H_2S and (b) 5 ppm H_2S.

Table 2
Comparison of the sensing performance of the present work and that of devices reported in the literature.

Sensing electrode	Working temperature (°C)	H_2S Concentration (ppm)	Response/Recovery time (s)	Low Detection Limit (ppm)	Ref.
La_2NiO_4	500	0.5	70/60	0.02	[59]
TiNT film	300	50	22/6	1	[60]
Ag- $CaCu_3Ti_4O_{12}$	250	10	5/850	0.2	[61]
α-Fe_2O_3	135	5	10/45	1	[62]
Ag–In_2O_3	25	20	84/186	0.005	[63]
NiO	25	48.5	6.54/9.5	0.485	[64]
Pt-Sn/C	25	50	10/8	0.2	Our work

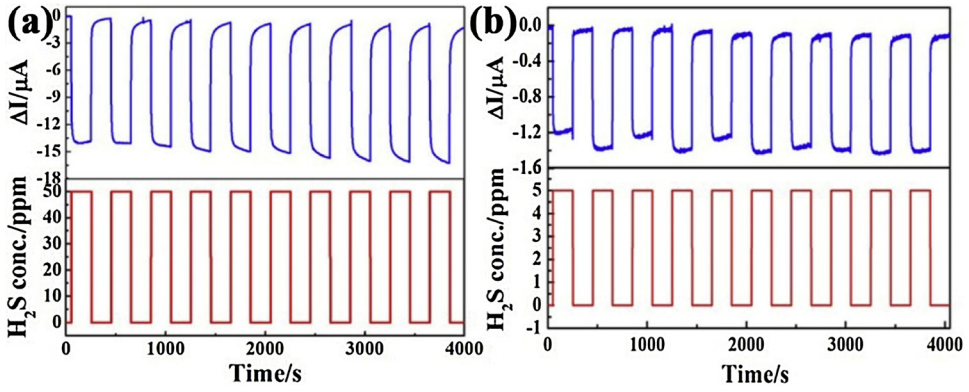

Fig. 9. The Continuous response-recovery curve of S_c to (a) 50 ppm H_2S and (b) 5 ppm H_2S.

constant value. At this point, the concentration of H_2S has reached saturation for the sensor. The response-recovery characteristics at low concentrations are shown in Fig. 7(b). The low detection limit is 0.2 ppm, which is 0.1 ppm higher than our previous work [35]. This is mainly because that the reaction of the gas at the sensing electrode is primarily controlled by the diffusion process at very low concentrations, and the most important factor affecting gas diffusion is the pore size of the electrode material. According to the BET test results, the average pore diameter of EM_c is 9.14 nm, which is 43% lower than the electrode material prepared in our previous work. The smaller the pore size, the tighter the particle packing is, which is not beneficial to the diffusion of gas molecules, and the response signal is also greatly

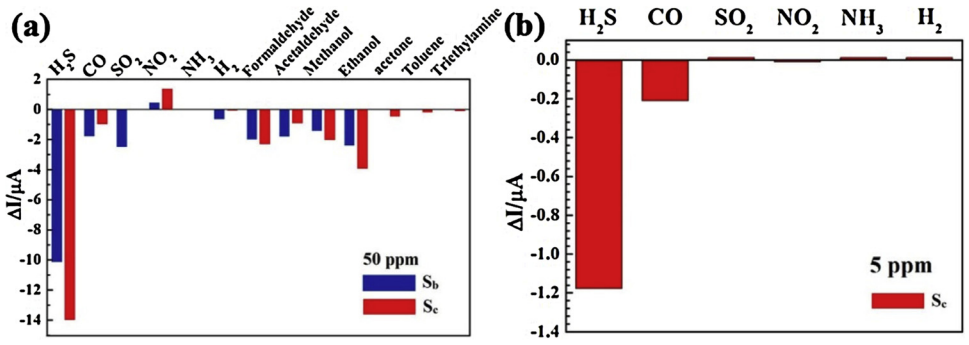

Fig. 10. Cross-sensitivity to various kinds of gases at a concentration of (a) 50 ppm and (b) 5 ppm.

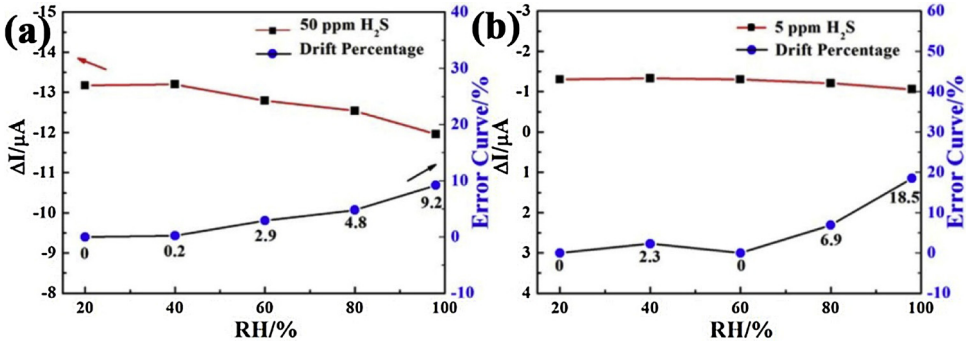

Fig. 11. Response current of S_c toward (a) 50 ppm H_2S and (b) 5 ppm H_2S at different relative humidity.

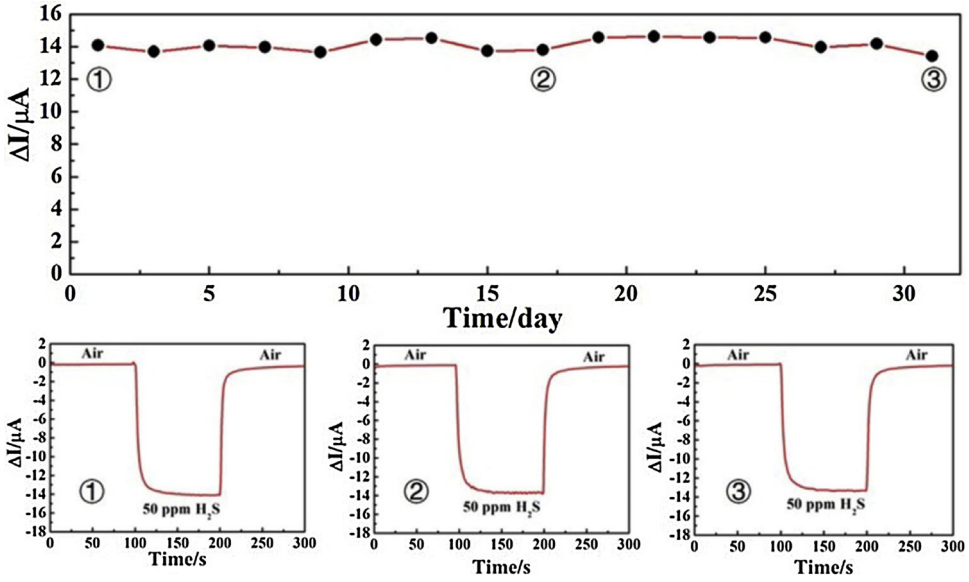

Fig. 12. Long-term stability of S_c toward 50 ppm H_2S.

affected at such low concentration, so the detection limit becomes high. When the concentration of H_2S is high, there are enough gas molecules to reach the active site, and the response signal is no longer controlled by the diffusion process. Although the low detection limit is slightly increased, the sensor can still detect low-concentration H_2S in extreme environments.

Current-time curves of the sensor to 50 ppm and 5 ppm H_2S are shown in Fig. 8. The response value of the sensor toward 50 ppm H_2S is 13.90 μA. As can be seen from the figure, the 90% response and recovery times to 50 ppm H_2S are 10 s and 8 s, and the times to 5 ppm H_2S are 11 s and 8 s, respectively. Such a short response-recovery time is a major advantage of the sensor. Due to the strong polarity of H_2S molecules, it is difficult to desorb on the surface of the electrode material. Obtaining such a good result is especially rare for H_2S sensors operating at room temperature. Table 2 gives the main performance of the H_2S sensor reported in the last two years. It can be seen that our paper performs well especially in terms of operating temperature and response-recovery time.

To further study the sensing performance, the continuous response-recovery curves to 50 ppm and 5 ppm H_2S are shown in Fig. 9. It can be seen from Fig. 9(a) that ΔI does not change significantly in the first six cycles. Starting from the seventh cycle, ΔI increases slightly, but the change is less than 15%. This is mainly because as the number of cycles increases, the response of the sensor takes longer to return to the initial

value (I_a). And in Fig. 9(b), the response to 5 ppm H_2S fluctuates slightly during the first five cycles but is very stable in subsequent tests. In summary, the sensor exhibits acceptable repeatability and can achieve continuous detection toward H_2S.

Selectivity is another important indicator. There, ΔIs of S_b and S_c to a variety of interfering gases (CO, SO_2, NO_2, NH_3, H_2, formaldehyde, acetaldehyde, methanol, ethanol, acetone, toluene, and triethylamine) are shown in the Fig. 10(a). For pure Pt, the addition of Sn significantly improves the selectivity of the sensor, especially the response to CO and SO_2. We also added the selectivity of the sensor at low concentrations (5 ppm) in Fig. 10(b). We can see that the ΔI of S_c to H_2S is significantly higher than others, which shows superior selectivity and has a good application prospect. According to Hsieh et al. [65], CO adsorption mainly occurs on Pt sites, while OH formation would take place preferentially on the Sn sites. Thus, the introduction of Sn offers one pathway to strip CO from the Pt-CO sites, thereby suppressing the response to CO. We speculate that the response to SO_2 is extremely low for similar reasons, and the detailed mechanism needs to be further discussed.

Fig. 11 shows the response currents of the sensor to 50 ppm and 5 ppm H_2S at different relative humidity. As RH increases, ΔI basically shows a decreasing trend. We speculate that this is because when the relative humidity is high, water molecules will affect the adsorption of H_2S on the surface of the electrode material. Here, the error curve% is calculated as follows: $\Delta I_{error}\% = |\Delta I\text{-}\Delta I_0|/\Delta I_0 \times 100\%$, where ΔI_0 and ΔI are the current values in the first cycle and in the given humidity, respectively. It can be seen that ΔI changes no more than 10% in the range of 20%–98% RH toward 50 ppm H_2S, which shows good humidity resistance. At low concentrations of H_2S, the amount of change in ΔI reaches 18.5%, which is something we need to improve in future work.

Long-term stability is another important indicator of whether a sensor can be commercialized. At the end of the work, ΔI of the sensor to 50 ppm H_2S over 31 days is given in Fig. 12. The responses were measured every other day. During the 31-day test period, we can see that the response of the sensor varies over a very narrow range and no significant decline is observed. The response-recovery curves of the sensor on days 1, 17, and 31 are also given. It can be seen that the response-recovery characteristics of the sensor hardly changed during the test period, which exhibited good stability.

4. Conclusion

To sum up, we compared the Pt/C prepared by the sodium borohydride reduction method and the ethylene glycol method and selected the latter to synthesize the Pt-Sn/C electrode material. The Pt-Sn/C was used for constructing the Nafion-based amperometric gas sensor to realize highly selective and stable H_2S detection at room temperature. The gas sensing measurement results showed that the low detection limit was 0.2 ppm, and the response value toward 50 ppm H_2S was 13.90 μA at room temperature. The typical 90% response-recovery time to 50 ppm H_2S was 10 s and 8 s. The sensor also exhibited good long-term stability, acceptable repeatability, and humidity resistance. During the 31-day test period, there was no significant decrease in the response of the sensor and the fluctuation was less than 9%. The response of the present device to H_2S was also much more than that of other interfering gases, which displayed superior selectivity. Therefore, based on the above results, we think this sensor present the significant potential application value in real-time monitoring of H_2S monitoring at room temperature.

Acknowledgments

This work was supported by the National Nature Science Foundation of China (Nos. 61831011, 61533021, and 61520106003), National Key R&D Program of China (No. 2016YFC0201002) and Program for Chang Jiang Scholars and Innovative Research Team in University (No. IRT-17R47), Application and Basic Research of Jilin Province (20130102010JC, 20190201276JC), STIRT-JLU (2017TD-07).

References

[1] B. Alizadeh, A. Telmadarreie, S.R. Shadizadeh, F. Tezhe, Investigating geochemical characterization of Asmari and Bangestan reservoir oils and the source of H_2S in the Marun oilfield, Petrol. Sci. Technol. 30 (2012) 967–975.
[2] L.D. Knight, S.E. Presnell, Death by sewer gas - case report of a double fatality and review of the literature, Am. J. Foren. Med. Pathol. 26 (2005) 181–185.
[3] C. Szabo, A timeline of hydrogen sulfide (H_2S) research: from environmental toxin to biological mediator, Biochem. Pharmacol. 149 (2018) 5–19.
[4] T.H. Milby, R.C. Baselt, Hydrogen sulfide poisoning: clarification of some controversial issues, Am. J. Ind. Med. 35 (1999) 192–195.
[5] Z.S. Hosseini, A.I. zad, A. Mortezaali, Room temperature H_2S gas sensor based on rather aligned ZnO nanorods with flower-like structures, Sens. Actuators B Chem. 207 (2015) 865–871.
[6] K. Diao, M. Zhou, J. Zhang, Y. Tang, S. Wang, X. Cui, High response to H_2S gas with facile synthesized hierarchical ZnO microstructures, Sens. Actuators B Chem. 219 (2015) 30–37.
[7] W. Nakla, A. Wisitsora-at, A. Tuantranont, P. Singjai, S. Phanichphant, C. Liewhiran, H_2S sensor based on SnO_2 nanostructured film prepared by high current heating, Sens. Actuators B Chem. 203 (2014) 565–578.
[8] N. Zhao, Z. Chen, W. Zeng, Enhanced H_2S sensor based on electrospun mesoporous SnO_2 nanotubes, J. Mater. Sci. - Mater. Electron. 26 (2015) 9152–9157.
[9] Z. Li, N. Wang, Z. Lin, J. Wang, W. Liu, K. Sun, Y.Q. Fu, Z. Wang, Room-temperature high-performance H_2S sensor based on porous CuO nanosheets prepared by hydrothermal method, ACS Appl. Mater. Interfaces 8 (2016) 20962–20968.
[10] L. Zhang, Z. Liu, L. Jin, B. Zhang, H. Zhang, M. Zhu, W. Yang, Self-assembly gridding α-MoO_3 nanobelts for highly toxic H_2S gas sensors, Sens. Actuators B Chem. 237 (2016) 350–357.
[11] Z.X. Jiang, J. Li, H. Aslan, Q. Li, Y. Li, M.L. Chen, Y.D. Huang, J.P. Froning, M. Otyepka, R. Zboril, F. Besenbacher, M.D. Dong, A high efficiency H_2S gas sensor material: paper like Fe_2O_3/graphene nanosheets and structural alignment dependency of device efficiency, J. Mater. Chem. A 2 (2014) 6714–6717.
[12] A. Stanoiu, C.E. Simion, J.M. Calderon-Moreno, P. Osiceanu, M. Florea, V.S. Teodorescu, S. Somacescu, Sensors based on mesoporous SnO_2-$CuWO_4$ with high selective sensitivity to H_2S at low operating temperature, J. Hazard. Mater. 331 (2017) 150–160.
[13] M. Kaur, B.K. Dadhich, R. Singh, KailasaGanapathi, T. Bagwaiya, S. Bhattacharya, A.K. Debnath, K.P. Muthe, S.C. Gadkari, RF sputtered SnO_2:NiO thin films as sub-ppm H_2S sensor operable at room temperature, Sens. Actuators B Chem. 242 (2017) 389–403.
[14] X. Liang, T.-H. Kim, J.-W. Yoon, C.-H. Kwak, J.-H. Lee, Ultrasensitive and ultraselective detection of H_2S using electrospun CuO-loaded In_2O_3 nanofiber sensors assisted by pulse heating, Sens. Actuators B Chem. 209 (2015) 934–942.
[15] B.-Y. Yeh, B.-S. Jian, G.-J. Wang, W.J. Tseng, CuO/V_2O_5 hybrid nanowires for highly sensitive and selective H_2S gas sensor, RSC Adv. 7 (2017) 49605–49612.
[16] H. Moser, W. Polz, J.P. Waclawek, J. Ofner, B. Lendl, Implementation of a quantum cascade laser-based gas sensor prototype for sub-ppmv H_2S measurements in a petrochemical process gas stream, Anal. Bioanal. Chem. 409 (2017) 729–739.
[17] A.Y. Mironenko, A.A. Sergeev, A.E. Nazirov, E.B. Modin, S.S. Voznesenskiy, S.Y. Bratskaya, H_2S optical waveguide gas sensors based on chitosan/Au and chitosan/Ag nanocomposites, Sens. Actuators B Chem. 225 (2016) 348–353.
[18] S. Viciani, M. Siciliani de Cumis, S. Borri, P. Patimisco, A. Sampaolo, G. Scamarcio, P. De Natale, F. D'Amato, V. Spagnolo, A quartz-enhanced photoacoustic sensor for H_2S trace-gas detection at 2.6 μm, Appl. Phys. B 119 (2014) 21–27.
[19] S.P. Fernandez Bordín, H.E. Andrada, A.C. Carreras, G.E. Castellano, R.G. Oliveira, V.M. Galván Josa, Nafion membrane channel structure studied by small-angle X-ray scattering and Monte Carlo simulations, Polymer 155 (2018) 58–63.
[20] K. Mochizuki, H. Iwatsu, M. Sudoh, Y. Ishiguro, T. Suzuki, Response properties of amperometric CO sensor using a polybenzimidazole (PBI) membrane above 140 degrees, Electrochemistry 78 (2010) 129–131.
[21] M.R. Rahman, J.T.S. Allan, M. Zamanzad Ghavidel, L.E. Prest, F.S. Saleh, E.B. Easton, The application of power-generating fuel cell electrode materials and monitoring methods to breath alcohol sensors, Sens. Actuators B Chem. 228 (2016) 448–457.
[22] Y. Guan, M. Dai, T. Liu, Y. Liu, F. Liu, X. Liang, H. Suo, P. Sun, G. Lu, Effect of the dispersants on the performance of fuel cell type CO sensor with Pt–C/Nafion electrodes, Sens. Actuators B Chem. 230 (2016) 61–69.
[23] Y. Guan, F. Liu, B. Wang, X. Yang, X. Liang, H. Suo, P. Sun, Y. Sun, J. Ma, J. Zheng, Y. Wang, G. Lu, Highly sensitive amperometric Nafion-based CO sensor using Pt/C electrodes with different kinds of carbon materials, Sens. Actuators B Chem. 239 (2017) 696–703.
[24] J.T.S. Allan, E.B. Easton, Polyvinyl chloride composite membranes made with Nafion and polysiloxanes for use in electrochemical breath alcohol sensors, J. Electrochem. Soc. 163 (2016) B644–B651.
[25] K. Mochizuki, A. Yamamoto, T. Kikuchi, M. Sudoh, Y. Gomi, Y. Ishiguro, T. Suzuki, Effects of electrode catalyst loading and membrane degradation for fuel cell type CO sensor, Sens. Lett. 9 (2010) 679–683.
[26] C.B. Yu, Y.J. Wang, K.F. Hua, W. Xing, H. Yang, T.H. Lu, Application of modified Nafion membrane to the sulfur dioxide gas electrochemical sensor, Chin. J. Anal. Chem. 30 (2002) 397–400.
[27] J. Zajda, N.J. Schmidt, Z. Zheng, X. Wang, M.E. Meyerhoff, Performance of amperometric platinized-Nafion based gas phase sensor for determining nitric oxide (NO) levels in exhaled human nasal breath, Electroanalysis 30 (2018) 1610–1615.
[28] Z. Zheng, H. Ren, I. VonWald, M.E. Meyerhoff, Highly sensitive amperometric Pt-

Nafion gas phase nitric oxide sensor: performance and application in characterizing nitric oxide-releasing biomaterials, Anal. Chim. Acta 887 (2015) 186–191.
[29] K. Ho, W. Hung, An amperometric NO_2 gas sensor based on Pt/Nafion® Electrode, Sens. Actuators B Chem. 79 (2001) 11–16.
[30] Y.-C. Liu, B.-J. Hwang, I.-J. Tzeng, Characteristics of solid-state amperometric oxygen sensor using Pt/C film hot-pressed onto Nafion membrane, Electroanalysis 13 (2001) 1441–1446.
[31] Y.-C. Liu, B.-J. Hwang, W.-C. Hsu, Characteristics of Pd/Nafion oxygen sensor modified with polypyrrole by chemical vapor deposition, J. Solid State Electrochem. 6 (2001) 351–356.
[32] Y.C. Liu, B.J. Hwang, I.J. Tzeng, Solid-state amperometric hydrogen sensor using Pt/C/Nafion composite electrodes prepared by a hot-pressed method, J. Electrochem. Soc. 149 (2002) H173–H178.
[33] Y.-C. Weng, K.-C. Hung, Amperometric hydrogen sensor based on Pt_xPd_y/Nafion electrode prepared by Takenata–Torikai method, Sens. Actuators B Chem. 141 (2009) 161–167.
[34] Y.-C. Weng, K.-C. Hung, J.-C. Wang, Y.-G. Lee, Y.-F. Su, C.-Y. Lin, Binary platinum–ruthenium/Nafion electrodes for the detection of hydrogen, Sens. Actuators B Chem. 150 (2010) 264–270.
[35] X. Yang, Y. Zhang, X. Hao, Y. Song, X. Liang, F. Liu, F. Liu, P. Sun, Y. Gao, X. Yan, G. Lu, Nafion-based amperometric H_2S sensor using Pt-Rh/C sensing electrode, Sens. Actuators B Chem. 273 (2018) 635–641.
[36] N. Jamalpoor, M. Ghasemi, V. Soleimanian, Investigation of the role of deposition rate on optical, microstructure and ethanol sensing characteristics of nanostructured Sn doped In_2O_3 films, Mater. Res. Bull. 106 (2018) 49–56.
[37] N. Singh, A. Umar, N. Singh, H. Fouad, O.Y. Alothman, F.Z. Haque, Highly sensitive optical ammonia gas sensor based on Sn Doped V_2O_5 Nanoparticles, Mater. Res. Bull. 108 (2018) 266–274.
[38] Y. Al-Hadeethi, A. Umar, S.H. Al-Heniti, R. Kumar, S.H. Kim, X. Zhang, B.M. Raffah, 2D Sn-doped ZnO ultrathin nanosheet networks for enhanced acetone gas sensing application, Ceram. Int. 43 (2017) 2418–2423.
[39] L.G. Martin, I. Green, X. Wang, S. Pasupathi, B.G. Pollet, Pt–Sn/C as a possible methanol-tolerant cathode catalyst for DMFC, Electrocatalysis 4 (2013) 144–153.
[40] F. Colmati, E. Antolini, E.R. Gonzalez, Pt–Sn/C electrocatalysts for methanol oxidation synthesized by reduction with formic acid, Electrochim. Acta 50 (2005) 5496–5503.
[41] S.C. Zignani, V. Baglio, J.J. Linares, G. Monforte, E.R. Gonzalez, A.S. Aricò, Endurance study of a solid polymer electrolyte direct ethanol fuel cell based on a Pt–Sn anode catalyst, Int. J. Hydrogen Energy 38 (2013) 11576–11582.
[42] S. Meenakshi, P. Sridhar, S. Pitchumani, Carbon supported Pt–Sn/SnO_2 anode catalyst for direct ethanol fuel cells, RSC Adv. 4 (2014) 44386–44393.
[43] S. Gómez-Quero, T. Tsoufis, P. Rudolf, M. Makkee, F. Kapteijn, G. Rothenberg, Kinetics of propane dehydrogenation over Pt–Sn/Al_2O_3, Catal. Sci. Technol. 3 (2013) 962–971.
[44] N. Kaylor, R.J. Davis, Propane dehydrogenation over supported Pt-Sn nanoparticles, J. Catal. 367 (2018) 181–193.
[45] S.S. Gwebu, P.N. Nomngongo, N.W. Maxakato, Pt-Sn nanoparticles supported on carbon nanodots as anode catalysts for alcohol electro-oxidation in acidic conditions, Electroanalysis 30 (2018) 1125–1132.
[46] D. González-Quijano, W.J. Pech-Rodríguez, J.I. Escalante-García, G. Vargas-Gutiérrez, F.J. Rodríguez-Varela, Electrocatalysts for ethanol and ethylene glycol oxidation reactions. Part I: effects of the polyol synthesis conditions on the characteristics and catalytic activity of Pt–Sn/C anodes, Int. J. Hydrogen Energy 39 (2014) 16676–16685.
[47] F.E. López-Suárez, A. Bueno-López, K.I.B. Eguiluz, G.R. Salazar-Banda, Pt–Sn/C catalysts prepared by sodium borohydride reduction for alcohol oxidation in fuel cells: effect of the precursor addition order, J. Power Sources 268 (2014) 225–232.
[48] M. Roca-Ayats, O. Guillén-Villafuerte, G. García, M. Soler-Vicedo, E. Pastor, M.V. Martínez-Huerta, PtSn nanoparticles supported on titanium carbonitride for the ethanol oxidation reaction, Appl. Catal. B-Environ. 237 (2018) 382–391.
[49] Christina Bock, Chantal Paquet, Martin Couillard, Gianluigi A. Botton, B.R. MacDougall, Size-Selected Synthesis of PtRu Nano-Catalysts: Reaction and Size Control Mechanism, (2004), pp. 8028–8037.
[50] E. Antolini, E.R. Gonzalez, A simple model to assess the contribution of alloyed and non-alloyed platinum and tin to the ethanol oxidation reaction on Pt–Sn/C catalysts: application to direct ethanol fuel cell performance, Electrochim. Acta 55 (2010) 6485–6490.
[51] V.I. Rodríguez, N.S. Veizaga, S.R. de Miguel, Effect of the preparation method on the electrocatalytic activity of Pt-Sn/nanotubes catalysts used in DMFC, J. Electrochem. Soc. 164 (2017) F1524–F1533.
[52] M. Gaidi, B. Chenevier, M. Labeau, Electrical properties evolution under reducing gaseous mixtures (H_2, H_2S, CO) of SnO_2 thin films doped with Pd/Pt aggregates and used as polluting gas sensors, Sens. Actuators B Chem. 62 (2000) 43–48.
[53] P.M. Bulemo, H.J. Cho, D.H. Kim, I.D. Kim, Facile synthesis of Pt-functionalized meso/macroporous SnO_2 hollow spheres through in situ templating with SiO_2 for H_2S sensors, ACS Appl. Mater. Interfaces 10 (2018) 18183–18191.
[54] C.M. Ghimbeu, M. Lumbreras, M. Siadat, R.C. van Landschoot, J. Schoonman, Electrostatic sprayed SnO_2 and Cu-doped SnO_2 films for H_2S detection, Sens. Actuators B Chem. 133 (2008) 694–698.
[55] K.-Y. Dong, J.-K. Choi, I.-S. Hwang, J.-W. Lee, B.H. Kang, D.-J. Ham, J.-H. Lee, B.-K. Ju, Enhanced H_2S sensing characteristics of Pt doped SnO_2 nanofibers sensors with micro heater, Sens. Actuators B Chem. 157 (2011) 154–161.
[56] W. Zhou, Pt based anode catalysts for direct ethanol fuel cells, Appl. Catal. B-Environ. 46 (2003) 273–285.
[57] P.E. Tsiakaras, PtM/C (M = Sn, Ru, Pd, W) based anode direct ethanol–PEMFCs: Structural characteristics and cell performance, J. Power Sources 171 (2007) 107–112.
[58] Z. Liu, B. Guo, L. Hong, T.H. Lim, Microwave heated polyol synthesis of carbon-supported PtSn nanoparticles for methanol electrooxidation, Electrochem. Commun. 8 (2006) 83–90.
[59] X. Hao, C. Ma, X. Yang, T. Liu, B. Wang, F. Liu, X. Liang, C. Yang, H. Zhu, G. Lu, YSZ-based mixed potential H_2S sensor using La_2NiO_4 sensing electrode, Sens. Actuators B Chem. 255 (2018) 3033–3039.
[60] X. Tong, W. Shen, X. Chen, J.-P. Corriou, A fast response and recovery H_2S gas sensor based on free-standing TiO_2 nanotube array films prepared by one-step anodization method, Ceram. Int. 43 (2017) 14200–14209.
[61] A. Natkaeo, D. Phokharatkul, J.H. Hodak, A. Wisitsoraat, S.K. Hodak, Highly selective sub–10 ppm H_2S gas sensors based on Ag-doped $CaCu_3Ti_4O_{12}$ films, Sens. Actuators B Chem. 260 (2018) 571–580.
[62] H.-J. Zhang, F.-N. Meng, L.-Z. Liu, Y.-J. Chen, Convenient route for synthesis of alpha-Fe_2O_3 and sensors for H_2S gas, J. Alloys Compd. 774 (2019) 1181–1188.
[63] S. Yan, Z. Li, H. Li, Z. Wu, J. Wang, W. Shen, Y.Q. Fu, Ultra-sensitive room-temperature H_2S sensor using Ag–In_2O_3 nanorod composites, J. Mater. Sci. 53 (2018) 16331–16344.
[64] W. Liu, J. Wu, Y. Yang, H. Yu, X. Dong, X. Wang, Z. Liu, T. Wang, B. Zhao, Facile synthesis of three-dimensional hierarchical NiO microflowers for efficient room temperature H_2S gas sensor, J. Mater. Sci. - Mater. Electron. 29 (2017) 4624–4631.
[65] C.-T. Hsieh, Y.-S. Chang, K.-M. Yin, Pt–Sn nanoparticles decorated carbon nanotubes as electrocatalysts with enhanced catalytic activity, J. Phys. Chem. C 117 (2013) 15478–15486.

Xinyu Yang received the B.Eng. degree in department of electronic science and technology in 2017. He is currently studying for his M.E. Sci. degree in College of Electronic Science and Engineering, Jilin University, China.

Weijia Li received the B.Eng. degree in department of microelectronics science and engineering in 2018. She is currently studying for her M.E. Sci. degree in College of Electronic Science and Engineering, Jilin University, China.

Yueying Zhang received the B.Eng. degree in department of electronic science and technology in 2017. She is currently studying for her M.E. Sci. degree in College of Electronic Science and Engineering, Jilin University, China.

Tong Liu received the B.Eng. degree in department of electronic science and technology in 2016. She is currently studying for her Ph.D. degree in College of Electronic Science and Engineering, Jilin University, China.

Xidong Hao received the B.Eng. degree in department of electronic science and technology in 2016. He is currently studying for his Ph.D. degree in College of Electronic Science and Engineering, Jilin University, China.

Ri Zhou received the Master of Science in department of chemistry in 2018. He is currently studying for his Ph.D. degree in College of Electronic Science and Engineering, Jilin University, China.

Xishuang Liang received the B. Eng. degree in department of electronic science and technology in 2004. He received his Doctor's degree in college of electronic science and engineering at Jilin University in 2009. Now he is a professor of Jilin University, China. His current research is solid electrolyte gas sensor.

Fengmin Liu received the B.E. degree in department of electronic science and technology in 2000. She received her Doctor's degree in college of electronic science and engineering at Jilin University in 2005. Now she is a professor in Jilin University, China. Her current research is preparation and application of semiconductor oxide, especial in gas sensor and solar cell.

Fangmeng Liu received his Ph.D. degree in 2017 from college of electronic science and engineering, Jilin University, China. Now he is a lecturer of Jilin University, China. His current research interests include the application of functional materials and development of solid state electrolyte gas sensor and flexible device.

Yuan Gao received her Ph.D. degree from Department of Analytical Chemistry at Jilin University in 2012. Now she is an associate professor in Jilin University, China. Her current research is focus on the preparation and application of graphene and semiconductor oxide, especial in gas sensor and biosensor.

Xu Yan received his M.S degree in 2013 from Nanjing Agricultural University. He joined the group of Prof. Xingguang Su at Jilin University and received his Ph.D. degree in June 2017. Since then, he did postdoctoral work with Prof. Geyu Lu. Currently, his research interests mainly focus on the development of the functional nanomaterials for chem/bio sensors.

Geyu Lu received the B.Sci. degree in electronic sciences in 1985 and the M.S.degree in 1988 from Jilin University in China and the Dr. Eng. degree in 1998 from Kyushu University in Japan. Now he is a professor of Jilin University, China. His current research interests include the development of chemical sensors and the application of the function materials.